SYNTHEGO | Full Stack Genome Engineering

Genome Edited iPS Cells. Guaranteed.

CRISPR-engineered iPS cells are enabling a new era in regenerative medicine. Physiologically relevant disease models lead to better discoveries and therapeutics.

Stem Cell Offerings

Knockout

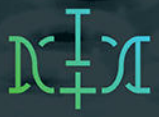

Single Nucleotide Variant

Tags

We offer knockouts, single nucleotide variants, and tag insertions in control or patient-derived iPS cell lines–available in homozygous or heterozygous clone or pool format.

Tell us about your project at

Synthego.com/SCTM

Synthego.com 1-844-4-CRISPR

STEM CELLS TRANSLATIONAL MEDICINE™

PROTOCOLS AND MANUFACTURING FOR CELL-BASED THERAPIES

Magnetic Resonance Imaging and Fluorescence Labeling of Clinical-Grade Mesenchymal Stem Cells Without Impacting Their Phenotype: Study in a Rat Model of Stroke

OLIVIER DETANTE,[a,b,c] SAMUEL VALABLE,[a,b] FLORENCE DE FRAIPONT,[b,d,e] EMMANUELLE GRILLON,[a,b] EMMANUEL LUC BARBIER,[a,b] ANAÏCK MOISAN,[a,b] JOSIANE ARNAUD,[b,f] CHRISTINE MORISCOT,[b,d,g] CHRISTOPH SEGEBARTH,[a,b] MARC HOMMEL,[b,h] CHANTAL REMY,[a,b] MARIE-JEANNE RICHARD[b,d,e,g]

Key Words. Mesenchymal stem cells • Cell migration • Cell culture • In vivo tracking

[a]Institut National de Santé et de Recherche Médicale, Grenoble, France; [b]Université Joseph Fourier, Grenoble, France; [c]Unité Neuro-Vasculaire, Neurologie, [d]Unité de Biochimie des Cancers et Biothérapies, [f]Biochimie Hormonale et Nutritionnelle, [g]Unité Mixte de Thérapie Cellulaire et Tissulaire, and [h]Institut National de Santé et de Recherche Médicale, Centre d'Investigation Clinique, Centre Hospitalier Universitaire de Grenoble, Grenoble, France; [e]Institut National de Santé et de Recherche Médicale, Institut Albert Bonniot, La Tronche, France

Correspondence: Olivier Detante, M.D., Ph.D., Grenoble Institut des Neurosciences, BP 170, 38042 Grenoble, Cedex 9, France. Telephone: 33-4-56-52-05-88; Fax: 33-4-56-52-05-98; e-mail: odetante@chu-grenoble.fr

Received October 21, 2011; accepted for publication February 29, 2012; first published online in SCTM *EXPRESS* April 2, 2012.

1066-5099/2012/$20.00/0

http://dx.doi.org/10.5966/sctm.2011-0043

ABSTRACT

Human mesenchymal stem cells (hMSCs) have strong potential for cell therapy after stroke. Tracking stem cells in vivo following a graft can provide insight into many issues regarding optimal route and/or dosing. hMSCs were labeled for magnetic resonance imaging (MRI) and histology with micrometer-sized superparamagnetic iron oxides (M-SPIOs) that contained a fluorophore. We assessed whether M-SPIO labeling obtained without the use of a transfection agent induced any cell damage in clinical-grade hMSCs and whether it may be useful for in vivo MRI studies after stroke. M-SPIOs provided efficient intracellular hMSC labeling and did not modify cell viability, phenotype, or in vitro differentiation capacity. Following grafting in a rat model of stroke, labeled hMSCs could be detected using both in vivo MRI and fluorescent microscopy until 4 weeks following transplantation. However, whereas good label stability and unaffected hMSC viability were observed in vitro, grafted hMSCs may die and release iron particles in vivo. STEM CELLS TRANSLATIONAL MEDICINE *2012;1:333–340*

INTRODUCTION

Stroke is the leading cause of acquired disability in human adults. There is currently no effective treatment after the acute stage. Thus, therapeutic strategies need to be developed to enhance brain plasticity after stroke onset. It has been shown that cell therapy can achieve this goal [1, 2].

Human mesenchymal stem cells (hMSCs) have strong clinical potential because they do not originate from a tumoral or a modified cell source [3] and are poorly immunogenic [4–6]. They can be used for cell therapy under autologous conditions after stroke [7, 8]. The use of hMSCs for tissue repair relies on their ability to survive long enough in the tissue of interest and to undergo differentiation into numerous cell types [9]. hMSCs have to be able to differentiate in vitro into chondrocytes, osteoblasts, and adipocytes. They can also differentiate into neurons [10, 11] and may promote structural and functional repairs in brain, in rodent models of stroke [5, 12–19].

Tracking labeled stem cells in vivo following local graft or i.v. injection can provide insight into many issues regarding optimal routing and/or dosing. hMSCs can be efficiently radiolabeled for nuclear imaging [20–27]. However, radiation-induced stem cell damage can then occur, notably on cell proliferation [25] and differentiation [28].

To avoid radiation damage, stem cells can be labeled for magnetic resonance imaging (MRI) with paramagnetic particles [29–31]. MRI-labeled stem cells have been detected in vivo, in animal models, in kidney [32, 33], in the heart [27, 34, 35], and in the brain [36–39]. Labeling may be achieved with superparamagnetic iron oxides (SPIOs). These are MRI contrast agents reducing signal intensity in T_2-weighted spin-echo (SE) and T_2*-weighted gradient-echo (GE) magnetic resonance (MR) images. They are thus sometimes called "negative" contrast agents in opposite to "positive" contrast agent (gadolinium chelates) [40]. SPIO contrast agents are particles composed of an iron-oxide core coated with dextran (ferumoxides) or carboxydextran (ferucarbotran). They also exist in the nanometer size (ultrasmall SPIOs [USPIOs], such as ferumoxtran) and in the micrometer size (micrometer-sized SPIOs [M-SPIOs]), such as iron fluorescent particles (IFPs; Bangs Laboratory, Fishers, IN,

http://www.bangslabs.com). IFPs contain a fluorophore enabling eventual histology and evaluation of labeling efficiency [31, 34, 41, 42].

To facilitate ex vivo stem cell labeling with USPIOs [38, 43] or with SPIOs [27, 35, 44–47], transfection agents are generally used. The deleterious effects of these agents on cells have not yet been fully investigated. Marked inhibition of chondrogenesis differentiation [46] and alteration of osteogenic differentiation [48] were observed after SPIO labeling of hMSCs, using transfection methods. SPIO labeling of hMSCs, without the use of transfection agents, was reported by Hsiao et al. [49]. Encouraging results were obtained in the attempt to detect hMSCs in vitro using MRI (1.5 T). The chondrogenic differentiation ability of the labeled cells was, however, not assessed in that study.

M-SPIOs coupled with a fluorescent marker, such as IFPs, have been used for MRI tracking of labeled macrophages intravenously injected in a rat model of brain tumor [42]. These particles modify neither the viability nor the differentiation ability of porcine MSCs [31]. Moreover, labeled porcine MSCs injected into infarcted myocardium of swine could be followed by MRI [34]. Given these limited data available about the effects of M-SPIOs on stem cells, these particles are not currently approved for clinical cell-therapy trials.

The aim of our study is thus to assess to what extent fluorescent M-SPIO labeling applied without transfection agent interacts with cell viability, proliferation, and differentiation of clinical-grade hMSCs and whether such labeling may be of interest for in vivo MRI cell tracking and histology in a rat model of stroke.

Materials and Methods

hMSC Culture

hMSCs were isolated from bone marrow aspirates of a healthy donor who gave informed consent. All of the isolation and culture procedures were conducted in the authorized Cell Therapy Unit (Biotherapy Team of General Clinical Research Center; French Health Minister agreement TCG/04/O/008/AA) at the Grenoble University Hospital. Clinical-grade hMSCs were produced according to a procedure of expansion approved by the French Health Products Safety Agency for the clinical trial (NCT00875654). The hMSCs were expanded in a fully closed system using the usual reagents (culture medium, trypsin, and fetal bovine serum) and materials. Quality controls were realized on the seeded bone marrow, during the process (at the first passage), and on the final harvested hMSCs. The quality controls included cell viability, hMSC identity (phenotypage), hMSC functionality (colony-forming fibroblast unit and in vitro differentiation in adipocytes, osteoblasts, and chondrocytes), tumorogenicity (soft-agar test and telomerase activity), and cytogenetic stability (karyotype).

The cells were cultured following the procedures previously described [6, 50]. Briefly, hMSCs were isolated following plastic adhesion, and they were then cultured at 37°C in a humidified atmosphere containing 5% CO_2. Minimum essential medium with α-modification (MEMα) was used, supplemented with 100 μg/ml penicillin, 100 μg/ml streptomycin, and 10% fetal calf serum (FCS) (all reagents from Invitrogen, Saint Aubin, France, http://www.invitrogen.com).

hMSC Magnetic Labeling with M-SPIOs (Iron Fluorescent Particles)

Early passage (second passage) hMSCs (50%–60% confluence) were incubated with M-SPIOs for 20 hours at 37°C in 5% CO_2. Twelve microliters (i.e., 76.1 μg of iron) of the M-SPIO solution (IFPs; Bangs Laboratory) was used per 75-cm^2 culture flask containing 6 ml of culture medium (i.e., 2 μl/ml; 12.7 μg of iron per ml). Particles (diameter = 0.9 μm; 63.4% magnetite, wt/wt) had a polydisperse carboxylated iron-oxide core and carried Dragon Green fluorophore (excitation wavelength = 480 nm; emission = 520 nm). After incubation, hMSCs were washed twice with phosphate-buffered saline (PBS) to remove the particles that had not been taken up and then cultured or trypsinated.

Labeling Efficiency, Cell Phenotype, and Viability

Labeling efficiency was assessed using epifluorescence microscopy and fluorescence-activated cell sorting (FACS) analysis (FACSCalibur; Becton, Dickinson and Company, Franklin Lakes, NJ, http://www.bd.com) on 25,000 cells. One and 4 days (two cell divisions) after M-SPIO labeling, hMSCs were immunophenotyped by FACS. The cells were detached with trypsin-EDTA, washed in PBS, and immediately stained with the following labeled antibodies: CD45-cychrome, CD73-PE, CD90-PE, and CD105-PE (BD Pharmingen, Franklin Lakes, NJ, http://www.bdbiosciences.com).

Flow cytometry was also used to check viability of the labeled cells using 7-aminoactinomycin D (7-AAD; BD Pharmingen). To evaluate the in vitro stem cell proliferation of labeled hMSCs, we performed a colony forming assay.

Cell Iron Content

The iron content of labeled and unlabeled (control) hMSCs was measured on three different hMSC cell cultures. Two days after hMSC labeling, the cells were washed three times with 0.9% NaCl and mineralized, for about 12 hours, in 30% HCl at 120°C. Iron concentration of the cell lysate was measured using inductible coupled plasma/atomic absorption spectroscopy (28270 spectrometer; Hitachi, Tokyo, http://www.hitachi.com/).

hMSC Differentiation

To define functional capacities of hMSCs as required for clinical use, we assessed in vitro adipocyte, chondrocyte, and osteoblast differentiations of labeled and unlabeled hMSCs. To induce adipocyte differentiation, hMSCs (labeled as well as unlabeled) were plated at 20,000 cells per cm^2 in 12-well plates, in MEMα containing 10% FCS, 1 μM dexamethasone, 10 μg/ml insulin, 0.5 mM 3-isobutyl-1-methylxanthine, and 100 μM indomethacin (Sigma, Saint Quentin Fallavier, France, http://www.sigmaaldrich.com). The medium was changed twice a week. After 3 weeks of adipogenic stimulation, the cells were rinsed once with PBS, fixed for 2 minutes with methanol at −20°C, rinsed with 50% ethanol, incubated for 10 minutes with Red Oil to stain lipid vacuoles, and rinsed again with 50% methanol.

To induce osteoblast differentiation, hMSCs were cultured in MEMα with 10% FCS, 10 mM β-glycerophosphate, 10^{-7} M dexamethasone, and 0.1 mM ascorbic acid. The medium was changed twice a week. After 3 weeks, the cells were fixed for 2 minutes with methanol at −20°C and washed for 10 minutes in 100 mM Tris, pH 9.5, 100 mM NaCl, and 10 mM $MgCl_2$ buffer. The cells

were then stained for 5–10 minutes with 5-bromo-4-chloro-3-indolyl phosphate/nitro blue tetrazolium (Sigma) and rinsed with distilled water.

For chondrogenesis, hMSCs were differentiated in a high-density pellet culture (2.5×10^6 cells per pellet) in MEMα supplemented with 10^{-7} M dexamethasone, 0.17 mM ascorbic acid, 40 μg/ml L-proline, 1 mM sodium pyruvate, 1× insulin, transferrin, sodium selenite, linoleic acid, and 10 ng/ml transforming growth factor-β3. After 3 weeks, with medium changes twice a week, the cell pellets were cryosectioned at 10-μm thickness, fixed with 4% paraformaldehyde, stained 2 hours with 0.5% Alcian Blue in 0.1 N HCl, and rinsed with distilled water.

Animal Model of Stroke

Animal procedures conformed to the French guidelines (Researcher License 380806 for O.D. and A3851610008 for animal care facilities). Anesthesia was induced by 5% isoflurane (Forène; Abbott Animal Health, Abbott Park, IL, http://www.abbottanimalhealth.com) in 30% O_2 and 70% air and maintained throughout the procedure with 2% isoflurane in a facial mask. Rectal temperature was maintained at 37.0 ± 0.5°C with an electrical heating blanket (water blanket for MRI) connected to a rectal probe.

Transient focal brain ischemia was induced by intraluminal middle cerebral artery occlusion (MCAo) [51, 52] in 14 adult Sprague-Dawley male rats (Janvier, Le Genest-Saint-Isle, France) weighing 300 g. Briefly, a cylinder of melted adhesive (length = 2 mm, diameter = 0.38 mm) attached to a nylon thread (diameter = 0.22 mm) was pushed from the lumen of the right external carotid artery into the internal carotid artery, up to 5 mm after the skull base. The rats were then awakened, and the thread was left in place for 90 minutes. The rats were tested for spontaneous circling and forelimb flexion during this occlusion period. After 90 minutes, the rats were reanesthetized, and the thread was removed.

Intracerebral Grafting and Experimental Groups

At day 1 (D1) after MCAo, the rats were randomly separated into two groups: treated rats ($n = 7$), which were grafted with an intracerebral (IC) injection of 400,000 labeled hMSCs (resuspended in 10 μl of 2 mM PBS-glutamine) into the damaged hemisphere, and control rats ($n = 7$), which received an IC injection of PBS-glutamine (cell suspension medium, 10 μl). The rats were fixed in a stereotaxic frame. Using a 25-gauge Hamilton (Reno, NV, http://www.hamiltoncompany.com) syringe, 7 μl of hMSC suspension (or PBS-glutamine) was injected into the right striatum (0 mm anteroposteriorly from bregma; 3 mm laterally; 6 mm deep) [53], and 3 μl was injected into the right cortex (0 mm anteroposteriorly from bregma; 3 mm laterally; 2 mm deep) at 1 μl/minute. No immunosuppressant was administrated.

Behavioral Tests and Follow-Up

To assess functional effects of the hMSC grafts, the rats were subjected to somatosensory tests that are widely used in stroke models: the modified neurological severity score (mNSS) and the adhesive removal test (ART) [14, 19]. The mNSS rates a combination of motor, sensory, balance, and reflex tests, between 0 (normal) and 18 (maximal deficit). The ART scores the time needed by the rat to remove two adhesive-backed paper dots (1 cm^2) applied on its wrists. To establish this score, three such experiments were done, separated by at least 5 minutes.

The rats were familiarized with the testing environment and trained for 3 days before surgery. ART and mNSS were assessed at D2, D7, D14, and D21 after MCAo. The data were expressed as the means ± SD. A repeated measure analysis of variance was applied after the homogeneity-of-variance hypothesis was tested (Levene test). A p value below .05 was considered significant.

In Vivo Brain MRI

MRI experiments were conducted at 2.35 T (horizontal magnet; Surrey Medical Imaging System Console). Immediately after MCAo (D0), the ischemic lesion was assessed using SE and SE diffusion-weighted MRI (SE-DW; repetition time/echo time [TR/TE] = 2,000/80 milliseconds, voxel size = 234 × 234 × 1,000 μm^3, $b = 700$ seconds/mm^2, two averages). The ischemic lesion was manually delineated on the SE-DW images obtained at D0. Lesion volumes were calculated by multiplying the number of pixels by pixel surface area and slice thickness.

After hMSC transplantation, SE-DW, SE MRI, and GE T_2*-weighted MRI (TR/TE = 400/25 milliseconds, voxel size = 234 × 234 × 469 μm^3, one average) were performed at D1, D15, and D28. The MRI sessions lasted approximately 40 minutes per rat.

Histology

At D1, D15, and D28, whole brains were removed after decapitation under isoflurane anesthesia, stored at −80°C, and cut using a cryostat (10-μm sections). Transplanted hMSCs were identified with a human-specific monoclonal antibody to nuclear antigen (MAB1281; 1/2,000; Chemicon, Temecula, CA, http://www.chemicon.com). This primary antibody was incubated overnight at 4°C before the tetramethylrhodamine B isothiocyanate-fluorescent anti-mouse secondary antibody (1/500; Jackson Laboratory, Bar Harbor, ME, http://www.jax.org) was applied for 1 hour. The green fluorescence of M-SPIO (IFP) labeling was directly visualized and all cell nuclei were counterstained blue with Hoechst prior to examination under microscopy (Eclipse E600; Nikon, Tokyo, http://www.nikon.com).

Results

hMSC Labeling and Viability

Preliminary experiments (exposure times from 30 minutes to 20 hours, with different concentrations of M-SPIO; data not shown) indicated the need for a long exposure of the hMSCs to M-SPIO to load cytoplasm with these particles. Therefore, we exposed hMSCs to M-SPIO for 20 hours, resulting in high-efficiency cell labeling without any modification of the cell's appearance (Fig. 1A). Fluorescent microscopy analysis indicated a cytoplasmic accumulation of the particles (Fig. 1A). Flow cytometry data showed that 1 day after M-SPIO labeling, 99% of the hMSCs were efficiently labeled and that 4 days later after two cell divisions, they remained labeled (Fig. 1B). Two days after cell labeling, iron concentration was 32.6 ± 10.1 nmol (1.8 ± 0.6 μg) in the lysate of 10^6 labeled hMSCs (corresponding to 1.8 pg or 6.6 IFPs per cell) versus 0.5 ± 0.1 nmol (0.03 μg) in the lysate of 10^6 unlabeled control hMSCs (0.03 g per cell).

Cell viability (flow cytometry with 7-AAD) remained stable following IFP labeling (Fig. 1C). The percentage of dead cells was 7.6% for control hMSCs and 5.1% for IFP-labeled hMSCs. The hMSC capacity to form colonies was similar for labeled (30 colony-forming units [CFUs] per 100 cells) and unlabeled cells (29 CFUs per 100 cells).

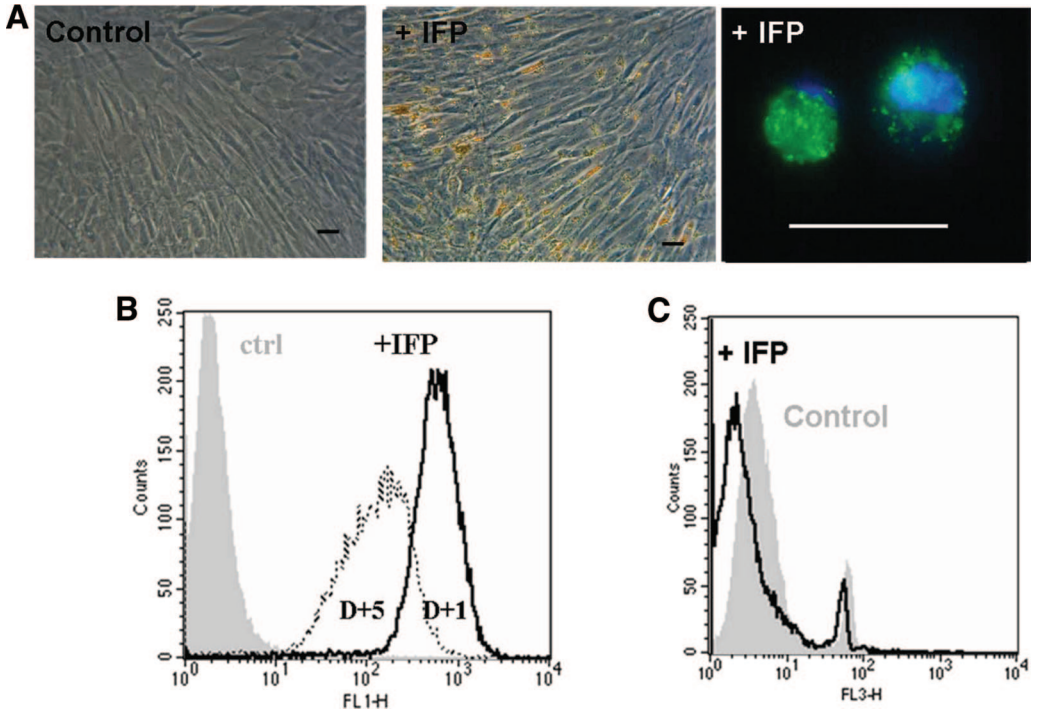

Figure 1. Micrometer-sized superparamagnetic iron oxide (M-SPIO) labeling of human mesenchymal stem cells (hMSCs) without transfection agent. **(A):** The iron content of M-SPIOs was observed by light microscopy and confirmed by fluorescence (M-SPIO in green and Hoechst counterstained in blue), indicating a cytoplasmic M-SPIO accumulation. **(B):** Flow cytometric analysis. One day after M-SPIO labeling (with iron fluorescent particles), 99% of cells contained particles, which remained labeled 4 days later, after two cell divisions. The decrease in fluorescence intensity corresponds to the redistribution of particles during cell divisions. **(C):** Flow cytometric analysis of cell viability (7-aminoactinomycin D) showing that cell viability was not affected by M-SPIO labeling. Scale bars = 50 μm. Abbreviations: ctrl, control; D+1, 1 day after M-SPIO labeling; D+5, 5 days after M-SPIO labeling; +IFP, with iron fluorescent particles.

Labeled hMSC Phenotype and Differentiation

M-SPIO labeling did not affect the baseline characteristics of the hMSCs (Fig. 2). More than 96% of labeled hMSCs expressed CD73, CD90, and CD105, whereas they did not express hematopoietic markers, such as CD45.

M-SPIO labeling did not significantly affect the capacity of hMSCs to differentiate into adipocytes, osteoblasts, and chondrocytes. Lipid vesicles, alkaline-phosphatase activity, and collagen II could be detected in labeled as well as unlabeled cells (Fig. 3).

Functional Effects of Intracerebral hMSC Grafts

All of the rats exhibited neurological deficits during the artery occlusion period (90 minutes). No adverse event was observed in both groups during the 3-week follow-up. Somatosensory recovery was better for the grafted group than for the control group. Significant benefit was observed according to ART (mean $\pm$ SD; treated group vs. control: D2, 67.6 $\pm$ 47.5 vs. 95.2 $\pm$ 24.1 seconds; D7, 61.7 $\pm$ 45.6 vs. 65.7 $\pm$ 36.8 seconds; D14, 41.5 $\pm$ 33.3 vs. 58.0 $\pm$ 41.1 seconds; and D21, 45.9 $\pm$ 30.7 vs. 63.0 $\pm$ 46.2 seconds; $p = .031$). No significant difference was noted for mNSS (treated group vs. control: D2, 9.3 $\pm$ 5.6 vs. 6.9 $\pm$ 4.1; D7, 4.9 $\pm$ 3.5 vs. 3.0 $\pm$ 2.0; D14, 3.3 $\pm$ 3.0 vs. 4.0 $\pm$ 2.8; D21, 3.3 $\pm$ 1.5 vs. 3.6 $\pm$ 1.8).

In Vivo MRI Cell Tracking

Immediately after MCAo and before hMSC grafting (D0), SE-DW MR images revealed a right corticostriatal lesion in all rats

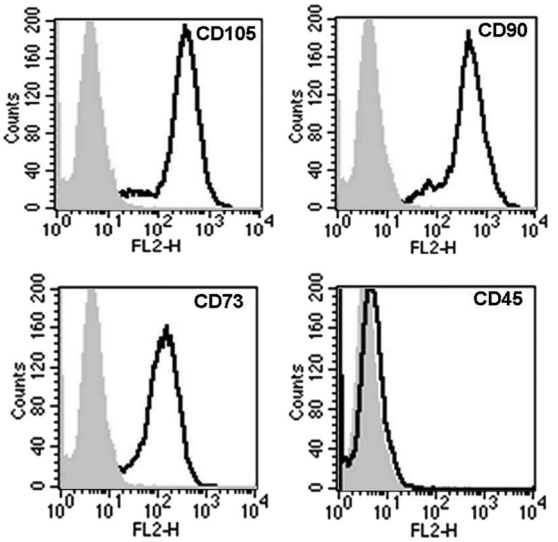

Figure 2. Phenotype of human mesenchymal stem cells (hMSCs) after micrometer-sized superparamagnetic iron oxide (M-SPIO) labeling. The cells were harvested and labeled with antibodies against CD45, CD73, CD90, CD105, or control IgGs as indicated and analyzed by fluorescence-activated cell sorting. Plots show isotype control IgG-staining profile (gray) versus specific antibody staining profile (thick line). More than 96% of the labeled cells expressed CD73, CD90, and CD105 and did not express the hematopoietic marker CD45. M-SPIO (iron fluorescent particle) labeling did not modify the phenotype of the hMSCs.

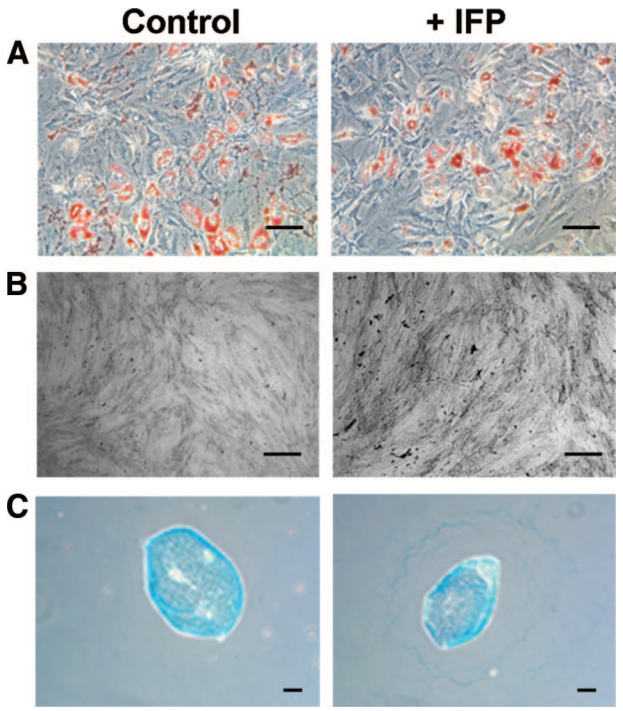

Figure 3. Human mesenchymal stem cell (hMSC) differentiation capacity after micrometer-sized superparamagnetic iron oxide (M-SPIO) labeling. Differentiation ability was assessed on control and labeled (+IFP) hMSCs. **(A):** Red Oil staining of the lipid vesicles performed 3 weeks after adipogenic stimulation demonstrates an ongoing adipogenesis. **(B):** Alkaline-phosphatase activity detected by 5-bromo-4-chloro-3-indolyl phosphate staining performed 3 weeks after osteogenic differentiation. **(C):** Collagen II detection with Alcian Blue after chondrogenic differentiation. M-SPIO (IFP) labeling did not significantly affect adipogenesis, osteogenesis, or chondrogenesis. Scale bars = 25 μm. Abbreviation: +IFP, with iron fluorescent particles.

(volume = 109 ± 64 mm^3). GE T_2*-weighted MR images did not reveal any hemorrhage.

Following hMSC grafting, labeled cells were detected at D1, D15, and D28 after MCAo in injection sites (right damaged striatum and cortex) (Fig. 4). Iron particles induced a magnetic susceptibility artifact (signal void) in the T_2* MR images, preventing us from determining lesion volume, after grafting.

Histology

Merging cellular images from human nuclei and cytoplasmic green fluorescence allowed us to observe, over the course of the experiment (until D28), viable labeled human cells derived from hMSCs in the infarcted tissue around both injection sites (Fig. 4). M-SPIO concentration at the graft site decreased steadily over 28 days but remained detectable (Fig. 4).

Discussion

Our results indicate that (a) without using transfection agent, M-SPIOs (IFPs) provide an efficient intracellular labeling of clinical-grade hMSCs; (b) in vitro, these particles modify neither cell viability nor proliferation, phenotype, or differentiation; (c) following IC grafting after stroke, labeled hMSCs can be detected by both in vivo MRI and fluorescence microscopy; and (d) a functional benefit from the grafts was observed during the 3-week follow-up.

Efficient and Safe Cell Labeling

Cellular MRI is useful to study the ability to migrate of hMSCs before their use in clinical trials of cell therapy. MRI was successfully applied to track migration of SPIO-labeled MSCs that had been IC grafted [39, 54] or injected intra-arterially [47] or intravenously [39, 47].

hMSCs labeled with fluorescent M-SPIO can be detected in vivo by MRI and ex vivo by fluorescence microscopy. The latter imaging modality (microscopy) permits assessment of the intracellular particle location after grafting. The former imaging modality (MRI) allows the detection of few cells, because of the large iron core of these particles strongly affecting the homogeneity of the static magnetic field [55–57].

Simply adding the iron particles to the culture medium (4.7×10^7 particles per milliliter; i.e., 2 μl/ml), we achieved nearly 100% labeling of clinical-grade hMSCs. Mean iron content per cell was approximately 1.8 pg (or 6.6 particles), less than what has been obtained with monocytes/macrophages labeled with a similar method (2.9 pg per cell) [42]. Also, without the use of transfection, labeling performance with a nonfluorescent SPIO in rat MSCs was 17.5 pg per cell after 72 hours of incubation [39], whereas with ferucarbotran in hMSCs it was 23.4 pg per cell after 24 hours of incubation [49]. When labeling porcine MSCs with a M-SPIO similar to that used in our study (IFPs), larger cell iron contents were reported over a significant range (20–380 pg per cell after 18 hours of incubation of 10 μl of IFPs per ml of medium). A more concentrated IFP solution was therefore used (23.5×10^7 particles/ml) [34]. The level of M-SPIO labeling of hMSCs, weaker than that of porcine MSCs or macrophages, might be ascribed to a lower phagocytic ability. To our knowledge, no study has reported direct comparisons between M-SPIO-labeled stem cell types.

After multiple cell divisions (in vitro hMSC doubling time = 50 hours), M-SPIO distributed well among daughter cells. hMSCs were still labeled after 4 days in culture medium. The decrease of fluorescence intensity reflects redistribution of the particles during cell divisions. Similar results were reported in other studies: a progressive decrease of fluorescence per cell over time consistent with porcine MSC divisions [31] or the detection of single-cell-stage mouse embryos following a large number of cell divisions [41]. These converging results open interesting prospects regarding in vivo tracking of proliferative cell populations.

Despite iron uptake, phenotype, proliferation, and differentiation potential of hMSCs remained unaffected and led to a functional benefit after stroke. Using larger M-SPIOs (1.63-μm diameter) for rat MSC labeling, Nohroudi et al. [57] showed that 2 μl of M-SPIO per milliliter of culture medium (as used in our study) was a "subcritical" dose, providing a preservation of cell function and migration and a sufficient MRI contrast. In contrast, higher concentrations (5 or 25 μl/ml) altered cell viability and migratory potential of labeled MSCs. This suggests that "as much as possible" labeling is not useful and could lead to cell necrosis and biased results for in vivo studies.

The labeling method with a subcritical dose and without using a transfection agent appears safe. It presents the advantage of great simplicity. Transfection labeling procedures, in contrast, appear to alter hMSC chondrogenesis [46] and osteogenic differentiation [48]. We therefore conclude that simple labeling methods without transfection have to be preferred in future cell therapy experiments. Moreover, as suggested for USPIO labeling of

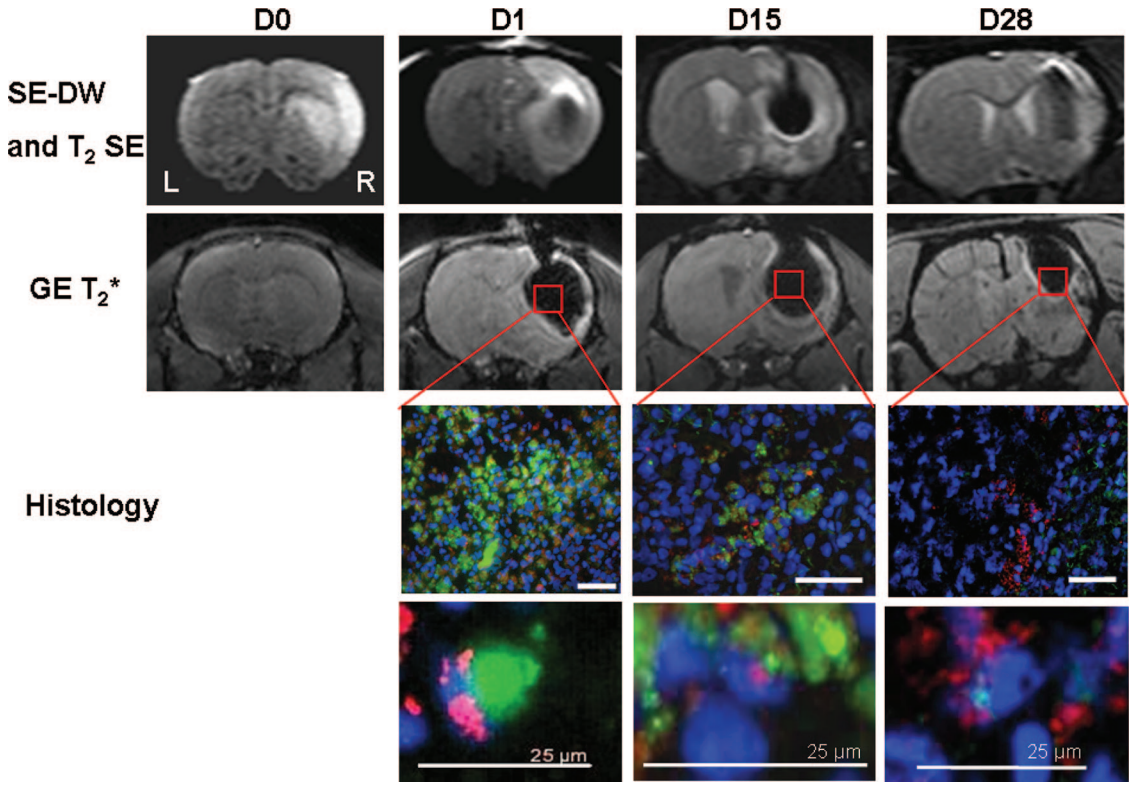

Figure 4. Labeled human mesenchymal stem cell (hMSC) detection by in vivo magnetic resonance imaging (MRI) and histology. Immediately after middle cerebral artery occlusion (D0), SE-DW images (first row) revealed the right corticostriatal ischemic lesion without any hemorrhage on gradient echo T_2*-weighted image (second row). After hMSC intracerebral grafting, at D1, D15, and D28, labeled cells were identified in vivo into both sites of injection (right damaged striatum and cortex) using SE-DW and T_2* imaging. A magnetic susceptibility artifact is seen as a signal void (dark area) on T_2* images caused by iron particles. For fluorescence microscopy, all of the cell nuclei were counterstained blue with Hoechst. Micrometer-sized superparamagnetic iron oxide (M-SPIO) green fluorescence is directly visualized and merged with a human-specific antibody to nuclear antigen (MAB1281) to identify human cells derived from hMSCs (in red). High-magnification images (bottom two rows) show the colocalization of this staining, corresponding to the presence of viable human cells with intracellular M-SPIO labeling at every time. M-SPIO concentration in the graft sites decreased for 28 days but remained notably detectable by MRI at D28. Scale bars = 50 μm (or 25 μm as noted). Abbreviations: D, day; DW, diffusion-weighted; GE, gradient echo; L, left; R, right; SE, spin echo.

mouse MSCs [58], it is necessary to assess the labeling efficiency but also the viability and the complete phenotype of labeled cells for each new contrast agent and each cell type.

Cell Tracking

SPIOs decrease T_2* and provide marked signal loss on T_2* GE MR images. The sensitivity of T_2* GE MRI allows detecting as little as a few labeled cells [41]. This high detection sensitivity is particularly useful to observe cell migration following intra-arterial [47] or i.v. [39] stem cell injections in stroke models. Because of their larger size, the magnetic susceptibility effects in the MR images are stronger with M-SPIOs than with SPIO nanoparticles (ferumoxides) [31], leading to a decreased cell detection threshold. The strong magnetic susceptibility effects of M-SPIOs induce an important signal void and geometrical distortions in T_2* GE MR images, immediately after the IC graft (Fig. 4). These effects need to be carefully considered for MRI studies performed shortly after IC grafting. They weaken with time as a result of the progressive decrease of the M-SPIO concentration at the graft sites.

Our results indicate that M-SPIO-labeled hMSCs can be detected by MRI up to 28 days after IC grafting. This observation is in accordance with the results from a previous study on SPIO labeling of hMSCs grafted by the IC route [54].

When considering long-term follow-up of iron-labeled cells, the issue of in vivo label stability needs to be addressed. Although good label stability and unaffected hMSC viability are observed in vitro, grafted hMSCs may die and release iron particles in vivo. Released iron particles taken by other cells (such as by macrophages; data not shown) or remaining in the extracellular space are equally detected by MRI. Thus, histological analysis is needed to assess the intracellular location and/or the release of the particles. M-SPIOs therefore present the advantage of being fluorescent, allowing easy assessment under microscopy. For future experiments, it could be relevant to correlate the MRI images by the sensitive measure of a human gene in the brain by polymerase chain reaction [59]. Histological control furthermore permits detection of intracerebral hemorrhages that may occur after ischemia/reperfusion and that may also lead to signal loss (usually at the site of the lesion) in T_2*-weighted MR images [42].

Concerning potential side effects of the iron release, a concentration-dependent toxicity of SPIOs has been suggested, in vitro, at high concentration (300–500 μg/ml) on murine macrophages (viability reduced to 55%–65%) but not at lower concentrations (25–200 μg/ml) [60]. The initial increase in oxidative stress (after SPIO uptake by macrophages) seems to be only transient (less than 1 day) [61]. On brain structures, no cytotoxicity or proinflammatory effect of SPIOs was observed on brain-derived endothelial cells, microglial cells, and differentiating three-dimensional aggregates [62]. These data suggest that a low dose of

M-SPIO for ex vivo cell labeling is safe, although an in vivo release can occur.

Conclusion

Clinical-grade hMSCs can be labeled by fluorescent M-SPIO particles without using any transfection agents. This simple method yields stable labeling without affecting hMSC viability, phenotype, and differentiation potential. Following IC grafting after stroke, labeled hMSCs can be detected both by in vivo MRI and by fluorescence microscopy. The hMSC grafting furthermore provides a functional benefit. Thus, this cell labeling method is useful to assess hMSC migration and homing in experimental studies of cell therapy.

Acknowledgments

O.D. was the recipient of an Institut National de Santé et de Recherche Médicale (INSERM) grant. This study was funded by an INSERM/Direction de l'Hospitalisation et de l'Organisation des Soins grant, by the Clinical Research Department of Grenoble University Hospital, and by the J. Fourier Grenoble University ("UJF-Vivier de la Recherche Médicale"). The authors thank the technical staffs of Grenoble Institut des Neurosciences Team Five and of the Cell Therapy Unit (Grenoble University Hospital) for their friendly technical support.

Author Contributions

O.D., S.V., F.d.F., and A.M., data collection and analysis, manuscript writing; E.G., J.A., and C.M., data collection; E.L.B., data analysis, manuscript correction; C.S. and C.R., manuscript writing; M.H. and M.-J.R., manuscript correction.

Disclosure of Potential Conflicts of Interest

The authors indicate no potential conflicts of interest.

References

1 Bliss T, Guzman R, Daadi M et al. Cell transplantation therapy for stroke. Stroke 2007;38:817–826.

2 Lindvall O, Kokaia Z. Stem cells for the treatment of neurological disorders. Nature 2006;441:1094–1096.

3 Jiang Y, Jahagirdar BN, Reinhardt RL et al. Pluripotency of mesenchymal stem cells derived from adult marrow. Nature 2002;418:41–49. Erratum in: Nature 2007;447:879–880.

4 Aggarwal S, Pittenger MF. Human mesenchymal stem cells modulate allogeneic immune cell responses. Blood 2005;105:1815–1822.

5 Li Y, Chen J, Chen XG et al. Human marrow stromal cell therapy for stroke in rat: Neurotrophins and functional recovery. Neurology 2002;59:514–523.

6 Plumas J, Chaperot L, Richard MJ et al. Mesenchymal stem cells induce apoptosis of activated T cells. Leukemia 2005;19:1597–1604.

7 Bang OY, Lee JS, Lee PH et al. Autologous mesenchymal stem cell transplantation in stroke patients. Ann Neurol 2005;57:874–882.

8 Lee JS, Hong JM, Moon GJ et al. A long-term follow-up study of intravenous autologous mesenchymal stem cell transplantation in patients with ischemic stroke. Stem Cells 2010;28:1099–1106.

9 Chamberlain G, Fox J, Ashton B et al. Concise review: Mesenchymal stem cells: Their phenotype, differentiation capacity, immunological features, and potential for homing. Stem Cells 2007;25:2739–2749.

10 Krampera M, Marconi S, Pasini A et al. Induction of neural-like differentiation in human mesenchymal stem cells derived from bone marrow, fat, spleen and thymus. Bone 2007;40:382–390.

11 Woodbury D, Schwarz EJ, Prockop DJ et al. Adult rat and human bone marrow stromal cells differentiate into neurons. J Neurosci Res 2000;61:364–370.

12 Borlongan CV, Lind JG, Dillon-Carter O et al. Bone marrow grafts restore cerebral blood flow and blood brain barrier in stroke rats. Brain Res 2004;1010:108–116.

13 Chen J, Li Y, Wang L et al. Therapeutic benefit of intravenous administration of bone marrow stromal cells after cerebral ischemia in rats. Stroke 2001;32:1005–1011.

14 Chen J, Li Y, Wang L et al. Therapeutic benefit of intracerebral transplantation of bone marrow stromal cells after cerebral ischemia in rats. J Neurol Sci 2001;189:49–57.

15 Chen J, Li Y, Katakowski M et al. Intravenous bone marrow stromal cell therapy reduces apoptosis and promotes endogenous cell proliferation after stroke in female rat. J Neurosci Res 2003;73:778–786.

16 Liu Z, Li Y, Qu R et al. Axonal sprouting into the denervated spinal cord and synaptic and postsynaptic protein expression in the spinal cord after transplantation of bone marrow stromal cell in stroke rats. Brain Res 2007;1149:172–180.

17 Onda T, Honmou O, Harada K et al. Therapeutic benefits by human mesenchymal stem cells (hMSCs) and Ang-1 gene-modified hMSCs after cerebral ischemia. J Cereb Blood Flow Metab 2008;28:329–340.

18 Shen LH, Li Y, Chen J et al. Therapeutic benefit of bone marrow stromal cells administered 1 month after stroke. J Cereb Blood Flow Metab 2007;27:6–13.

19 Shen LH, Li Y, Chen J et al. One-year follow-up after bone marrow stromal cell treatment in middle-aged female rats with stroke. Stroke 2007;38:2150–2156.

20 Allers C, Sierralta WD, Neubauer S et al. Dynamic of distribution of human bone marrow-derived mesenchymal stem cells after transplantation into adult unconditioned mice. Transplantation 2004;78:503–508.

21 Barbash IM, Chouraqui P, Baron J et al. Systemic delivery of bone marrow-derived mesenchymal stem cells to the infarcted myocardium: Feasibility, cell migration, and body distribution. Circulation 2003;108:863–868.

22 Bindslev L, Haack-Sorensen M, Bisgaard K et al. Labelling of human mesenchymal stem cells with indium-111 for SPECT imaging: Effect on cell proliferation and differentiation. Eur J Nucl Med Mol Imaging 2006;33:1171–1177.

23 Correa PL, Mesquita CT, Felix RM et al. Assessment of intra-arterial injected autologous bone marrow mononuclear cell distribution by radioactive labeling in acute ischemic stroke. Clin Nucl Med 2007;32:839–841.

24 de Haro J, Zurita M, Ayllon L et al. Detection of 111In-oxine-labeled bone marrow stromal cells after intravenous or intralesional administration in chronic paraplegic rats. Neurosci Lett 2005;377:7–11.

25 Detante O, Moisan A, Dimastromatteo J et al. Intravenous administration of 99mTc-HMPAO-labeled human mesenchymal stem cells after stroke: In vivo imaging and biodistribution. Cell Transplant 2009;18:1369–1379.

26 Gao J, Dennis JE, Muzic RF et al. The dynamic in vivo distribution of bone marrow-derived mesenchymal stem cells after infusion. Cells Tissues Organs 2001;169:12–20.

27 Kraitchman DL, Tatsumi M, Gilson WD et al. Dynamic imaging of allogeneic mesenchymal stem cells trafficking to myocardial infarction. Circulation 2005;112:1451–1461.

28 Brenner W, Aicher A, Eckey T et al. 111In-labeled CD34+ hematopoietic progenitor cells in a rat myocardial infarction model. J Nucl Med 2004;45:512–518.

29 Arbab AS, Pandit SD, Anderson SA et al. Magnetic resonance imaging and confocal microscopy studies of magnetically labeled endothelial progenitor cells trafficking to sites of tumor angiogenesis. Stem Cells 2006;24:671–678.

30 Bulte JWM, Kraitchman DL. Iron oxide MR contrast agents for molecular and cellular imaging. NMr Biomed 2004;17:484–499.

31 Hinds KA, Hill JM, Shapiro EM et al. Highly efficient endosomal labeling of progenitor and stem cells with large magnetic particles allows magnetic resonance imaging of single cells. Blood 2003;102:867–872.

32 Hauger O, Frost EE, van Heeswijk R et al. MR evaluation of the glomerular homing of magnetically labeled mesenchymal stem cells

in a rat model of nephropathy. Radiology 2006; 238:200–210.

33 Ittrich H, Lange C, Togel F et al. In vivo magnetic resonance imaging of iron oxide-labeled, arterially-injected mesenchymal stem cells in kidneys of rats with acute ischemic kidney injury: Detection and monitoring at 3T. J Magn Reson Imaging 2007;25:1179–1191.

34 Hill JM, Dick AJ, Raman VK et al. Serial cardiac magnetic resonance imaging of injected mesenchymal stem cells. Circulation 2003;108:1009–1014.

35 Kraitchman DL, Heldman AW, Atalar E et al. In vivo magnetic resonance imaging of mesenchymal stem cells in myocardial infarction. Circulation 2003;107:2290–2293.

36 Bulte JW, Zhang S, van Gelderen P et al. Neurotransplantation of magnetically labeled oligodendrocyte progenitors: Magnetic resonance tracking of cell migration and myelination. Proc Natl Acad Sci USA 1999;96:15256–15261.

37 Bulte JWM, Duncan ID, Frank JA. In vivo magnetic resonance tracking of magnetically labeled cells after transplantation. J Cereb Blood Flow Metab 2002;22:899–907.

38 Hoehn M, Kustermann E, Blunk J et al. Monitoring of implanted stem cell migration in vivo: A highly resolved in vivo magnetic resonance imaging investigation of experimental stroke in rat. Proc Natl Acad Sci USA 2002;99: 16267–16272.

39 Jendelová P, Herynek V, DeCroos J et al. Imaging the fate of implanted bone marrow stromal cells labeled with superparamagnetic nanoparticles. Magn Reson Med 2003;50:767–776.

40 Shyu W-C, Chen C-P, Lin S-Z et al. Efficient tracking of non-iron-labeled mesenchymal stem cells with serial MRI in chronic stroke rats. Stroke 2007;38:367–374.

41 Shapiro EM, Skrtic S, Sharer K et al. MRI detection of single particles for cellular imaging. Proc Natl Acad Sci USA 2004;101:10901–10906.

42 Valable S, Barbier EL, Bernaudin M et al. In vivo MRI tracking of exogenous monocytes/macrophages targeting brain tumors in a rat model of glioma. Neuroimage 2007;37(suppl 1):S47–S58.

43 Lewin M, Carlesso N, Tung CH et al. Tat peptide-derivatized magnetic nanoparticles allow in vivo tracking and recovery of progenitor cells. Nat Biotechnol 2000;18:410–414.

44 Arbab AS, Yocum GT, Kalish H et al. Efficient magnetic cell labeling with protamine sulfate complexed to ferumoxides for cellular MRI. Blood 2004;104:1217–1223.

45 Arbab AS, Yocum GT, Rad AM et al. Labeling of cells with ferumoxides-protamine sulfate complexes does not inhibit function or differentiation capacity of hematopoietic or mesenchymal stem cells. NMR Biomed 2005; 18:553–559.

46 Kostura L, Kraitchman DL, Mackay AM et al. Feridex labeling of mesenchymal stem cells inhibits chondrogenesis but not adipogenesis or osteogenesis. NMR Biomed 2004;17:513–517.

47 Walczak P, Zhang J, Gilad AA et al. Dual-modality monitoring of targeted intraarterial delivery of mesenchymal stem cells after transient ischemia. Stroke 2008;39:1569–1574.

48 Farrell E, Wielopolski P, Pavljasevic P et al. Effects of iron oxide incorporation for long term cell tracking on MSC differentiation in vitro and in vivo. Biochem Biophys Res Commun 2008;369:1076–1081.

49 Hsiao J-K, Tai M-F, Chu H-H et al. Magnetic nanoparticle labeling of mesenchymal stem cells without transfection agent: Cellular behavior and capability of detection with clinical 1.5 T magnetic resonance at the single cell level. Magn Reson Med 2007;58:717–724.

50 Moriscot C, de Fraipont F, Richard M-J et al. Human bone marrow mesenchymal stem cells can express insulin and key transcription factors of the endocrine pancreas developmental pathway upon genetic and/or microenvironmental manipulation in vitro. Stem Cells 2005;23:594–603.

51 Grillon E, Provent P, Montigon O et al. Blood-brain barrier permeability to manganese and to Gd-DOTA in a rat model of transient cerebral ischaemia. NMR Biomed 2008; 21:427–436.

52 Longa EZ, Weinstein PR, Carlson S et al. Reversible middle cerebral artery occlusion without craniectomy in rats. Stroke 1989;20: 84–91.

53 Paxinos G, Watson C. The Rat Brain in Stereotaxic Coordinates. San Diego: Academic Press, 1998.

54 Kim D, Chun B-G, Kim Y-K et al. In vivo tracking of human mesenchymal stem cells in experimental stroke. Cell Transplant 2008;16: 1007–1012.

55 Heyn C, Ronald JA, Mackenzie LT et al. In vivo magnetic resonance imaging of single cells in mouse brain with optical validation. Magn Reson Med 2006;55:23–29.

56 Shapiro EM, Sharer K, Skrtic S et al. In vivo detection of single cells by MRI. Magn Reson Med 2006;55:242–249.

57 Nohroudi K, Arnhold S, Berhorn T et al. In vivo MRI stem cell tracking requires balancing of detection limit and cell viability. Cell Transplant 2010;19:431–441.

58 Crabbe A, Vandeputte C, Dresselaers T et al. Effects of MRI contrast agents on the stem cell phenotype. Cell Transplant 2010;19:919–936.

59 Danchuk S, Ylostalo JH, Hossain F et al. Human multipotent stromal cells attenuate lipopolysaccharide-induced acute lung injury in mice via secretion of tumor necrosis factor-α-induced protein 6. Stem Cell Res Ther 2011;2:27.

60 Naqvi S, Samim M, Abdin M et al. Concentration-dependent toxicity of iron oxide nanoparticles mediated by increased oxidative stress. Int J Nanomedicine 2010;16:983–989.

61 Corot C, Robert P, Idée JM et al. Recent advances in iron oxide nanocrystal technology for medical imaging. Adv Drug Deliv Rev 2006; 58:1471–1504.

62 Cengelli F, Maysinger D, Tschudi-Monnet F et al. Interaction of functionalized superparamagnetic iron oxide nanoparticles with brain structures. J Pharmacol Exp Ther 2006;318: 108–116.